European Journal of Medicinal Chemistry 46 (2011) 3519–3525

Contents lists available at ScienceDirect

European Journal of Medicinal Chemistry

journal homepage: http://www.elsevier.com/locate/ejmech

Original article

Molecular modelling studies on Arylthioindoles as potent inhibitors of tubulin polymerization

Antonio Coluccia [a,*], Davide Sabbadin [b], Andrea Brancale [b]

[a] Istituto Pasteur — Fondazione Cenci Bolognetti, Dipartimento di Chimica e Tecnologie del Farmaco, Sapienza Università di Roma, Piazzale Aldo Moro 5, I-00185 Roma, Italy
[b] Welsh School of Pharmacy, Cardiff University, King Edward VII Avenue, Cardiff CF10 3NB, UK

ARTICLE INFO

Article history:
Received 3 March 2011
Received in revised form
2 May 2011
Accepted 8 May 2011
Available online 13 May 2011

Keywords:
Tubulin
Colchicine
Arylthioindole
Docking
Molecular dynamics

ABSTRACT

The crucial role played by microtubules in the life of eukaryotic cell makes tubulin an important route for the anticancer therapy. The Arylthioindoles (ATIs) along with the corresponding ketone and methylene compounds are potent tubulin assembly inhibitors. We are here reporting the result of a series of docking and molecular dynamics experiments on this series of compounds. The results obtained from our *in silico* studies not only provided us with an insight on the nature of the binding of the ATIs to tubulin, but were also at the core of the design of a new series of potent inhibitors of tubulin polymerization.

1. Introduction

The formation of microtubules is a dynamic process that involves the polymerization and depolymerization of α and β tubulin heterodimers. This process is tightly regulated: by the action of various regulatory proteins, by expression of different forms of the tubulin (in the human we know 6 forms for alpha-tubulin and 7 for beta-tubulin), by post-translational modification etc [1]. The large number of physiological control of the microtubules equilibrium is the consequence of its important role in the life of the eukaryotic cells [2]. Probably the most important role played by microtubules is during the mitosis, in the proper spindle function. Interference with microtubule assembly, either by inhibition of tubulin polymerization or by blocking microtubule disassembly, leads to an increase in the number of cells in metaphase arrest. Therefore targeting tubulin, as main component of the microtubules represents an important route to anticancer therapy.

A large number of chemically different compounds bind tubulin in the microtubules. The specific effects of each of them on the microtubules dynamics are complex and depend on the different binding site. All these compounds can be grouped in three different classes [Fig. 1]: a) taxol (**1**) group targets a lumenal site on the α-sub unit of tubulin dimers; b) vinblastine (**2**) group (not well characterized binding site), stimulates, and at high concentration, stabilizes microtubules polymerization; c) colchicine (**4**) group gets microtubules destabilization and subsequent cellular apoptosis binding at the interface between α and β subunits [3,4].

Regardless of the mechanism of action, clinical use of anti tubulin drugs is associated with problems of drug resistance, toxicity, and bioavailability [5]. For this reason, a considerable research effort in this field is currently underway to identify new potent inhibitors [6].

Among the novel anti tubulin structures proposed, we have identified the Arylthioindoles (ATIs Fig. 1) as a class of potent tubulin assembly inhibitors, which bind to the colchicine site [7–10]. ATIs efficiently inhibit tubulin polymerization and cancer cell growth, with activities comparable with those of colchicine (**4**) and CSA4 (**5**). The large number of ATIs synthesized so far has allowed us to devise a robust structure activity relationship (SAR) and the structural requirements: a) the methyl/ethyl ester function at position 2 of the indole; b) a small substituent at position 5 or 6 of the indole; c) a sulfur atom as bridge; d) a tri-methoxy substitution in positions 3, 4, 5 of the phenyl ring. With the amount of data now available on this class of compounds we are now in a position to rationalize the results obtained using a molecular modelling approach. Indeed, preliminary molecular docking

* Corresponding author. Tel.: +39 0644913404.
E-mail address: antonio.coluccia@uniroma1.it (A. Coluccia).

0223-5234/$ – see front matter © 2011 Elsevier Masson SAS. All rights reserved.
doi:10.1016/j.ejmech.2011.05.020

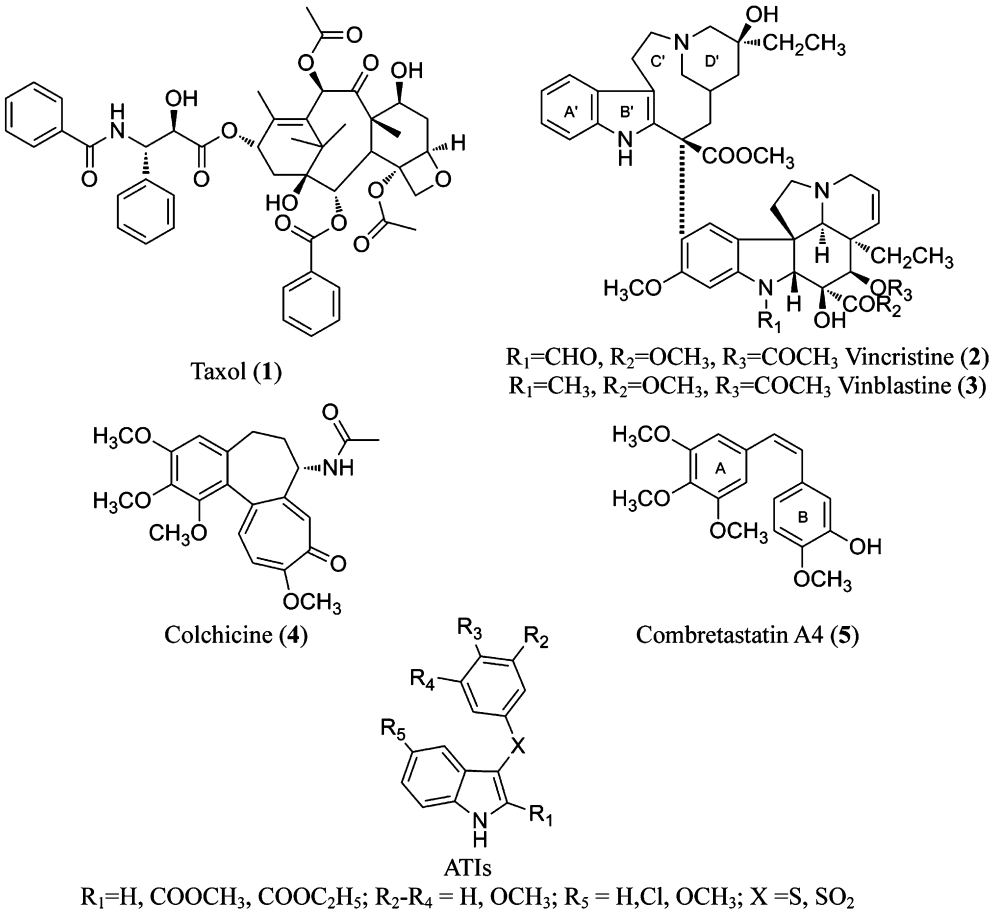

Fig. 1. Tubulin binding agents.

simulations have already suggested a possible binding mode for some of these compounds. With this in mind, we have performed an extensive molecular docking study and a series of molecular dynamics simulation of a selected number of ATIs (Table 1) with the aim of gaining a better understanding of the binding of these compounds to tubulin. Furthermore, results obtained have now been used to design a new, potent, series of compounds.

Table 1
Structures, inhibition of tubulin polymerization and calculated binding free energy.

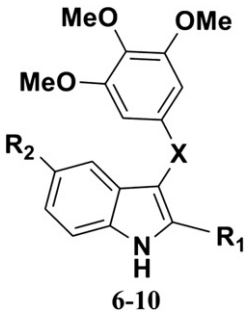

6-10

	R1	R2	X	IC_{50}[a] (μM)	ΔG[b] (kcal/mol)
6	COOMe	OMe	S	2.0	−8.22
7	COOMe	OMe	CH_2	1.4	−8.33
8	COOMe	OMe	CO	0.67	−9.64
9	Pyrrol-2-yl	H	S	1.1	−8.41
10	Thiophen-2-yl	H	S	0.74	−9.53
4				2.2	−8.15

[a] Inhibition of tubulin polymerization.
[b] Calculated free binding energy, kcal/mol.

2. Results and discussion

In our previous studies, we were able to identify a consistent binding mode of ATIs in the colchicine binding pocket. Nevertheless, the availability of new crystal structures of tubulin (PDB ID: 3HKC and 3HKE) [11] led us to evaluate what differences, if any, were observable in the binding mode of ATIs between these structures and the previously used complex tubulin/DAMA-colchicine (PDB ID 1SA0) [12].

Initial superimposition of the different tubulin structures revealed that generally there were no apparent significant differences between the structures. The major variations were related with the loops position as the rmsd of Cα for analyzed structures clearly show (Table 2). In particular the T5 [11] loop of the α sub unit formed by residues from Ala173α to Val181α showed a different conformation between 1SA0 and 3HKC/E structures. It is important to note that this loop plays an important role in the stabilization of both colchicine and ATIs in the binding site and for this reason we

Table 2
Carbon α rmsd between 3HKC, 3HKE and 1SA0 structures.

	3HKC	3HKE	1SA0		3HKC	3HKE	1SA0
3HKC	0	0.56	1.04	3HKC	0	0.37	0.47
3HKE	0.56	0	0.97	3HKE	0.37	0	0.51
1SA0	1.04	0.97	0	1SA0	0.47	0.51	0
Cα rmsd (Å) of tubulin α sub unit				Cα rmsd (Å) of tubulin β sub unit			

decided to perform molecular docking also on the more recent structures. In particular, due to limited differences between 3KHC and 3KHE structures and as a consequence of the dual binding mode of the 3HKE co-crystallized inhibitor [11], we decided to use only the 3HKC structure, along with 1SA0, in our simulations.

2.1. Molecular docking

We have previously [7–10] reported a series of molecular docking studies for different series of ATIs in the colchicine binding site of tubulin, using FlexX [13]. In these studies we have never observed a direct correlation between the scoring function and the biological activity experimentally recorded (inhibition of tubulin polymerization). Starting from these results, we explored the use of two other docking programs: PLANTS [14] and GLIDE [15] on a set of 94 ATIs analogues on which biological data was already available.

The analysis of docking results showed as both PLANTS and GLIDE placed the ATIs in the colchicine binding site in virtually the same conformation that we have described previously [7–10] with the tri-methoxy phenyl group in proximity of Cys241β, Leu248β and Leu255β; and forming a hydrogen bond between the indole NH and Thr179α. Also, no significant differences in the predicted poses of 1SA0 and 3HKC were identified.

As noted previously [9], we observed a dual binding mode for some derivatives. In particular, compound **6**, independently of the software or of the crystal structures used, presented two main clusters of poses: the best scored binding pose, as described above and a second one where the main difference was represented by the different orientation (180 degree rotation) of the indole nucleus. With this binding conformation the substituent in position 2 of the indole is located deeper in the binding pocket. Interestingly for both binding mode the key highlighted interactions were retained (Fig. 2).

As previously reported with FlexX, no correlation between the inhibition of tubulin polymerization data and the PLANTS scoring function was observed (data not shown). Interestingly, the GLIDE score performed slightly better, showing a modest correlation ($r^2 = 0.26$; Fig. 1S of Supporting Information), when the 1SA0 structure was used in the docking. Furthermore, when we examined the GLIDE score of specific groups of compounds based on the nature of the substituents on the indole ring, we noticed that when an halogen atom was present in the structure, the correlation between the score value and the biological activity was lost, possibly suggesting that the scoring function was not able to quantify accurately the impact of such substitutions. Indeed, when we removed the 36 halogenated compounds from our dataset, the correlation improved significantly ($r^2 = 0.47$; Fig. 1S of Supporting Information). It should be noted that the correlation is affected by the lack of precise activity values on the less active compound ($IC_{50} > 40$ μM).

Summarizing the docking poses obtained for the ATIs examined were consistent across the results obtained from the different docking programs and crystal structures. It is fair to say that no significant correlation was observed between the scoring values and the biological data and only a modest correlation was observed between the GLIDE score and the tubulin polymerization inhibition data, when the docking was performed using the 1SA0 tubulin structure.

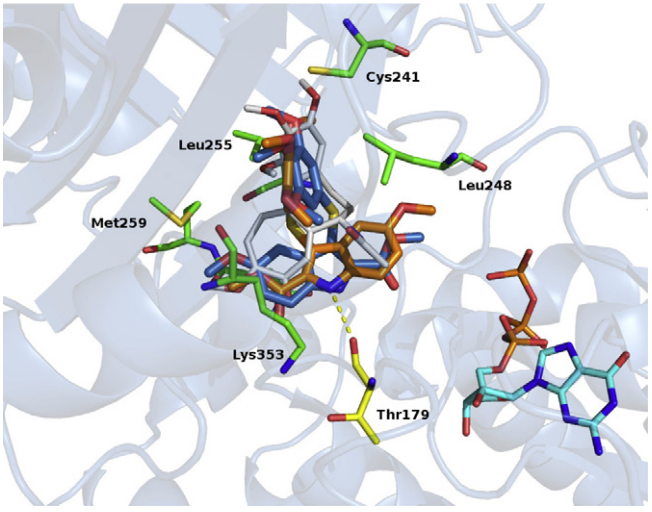

Fig. 2. Binding poses of derivative **6**, best scored in blue, second one in orange. Colchicine was reported as white lines. Tubulin was as cartoon representation. H-bonds are reported as dotted lines. α tubulin residues are reported in yellow; β tubulin residues are reported in green. (For interpretation of the references to colour in this figure legend, the reader is referred to the web version of this article.)

2.2. Molecular dynamic

To improve these results and possibly to gain some more information on the binding of the ATIs to tubulin, we have performed a series of molecular dynamics simulations on a series of selected compounds (Table 1), focusing our attention on the nature of the linker between the two aromatic rings (compounds **6**, **7** and **8**) and the role of the heterocycles in position 2 of the indole nucleus (compounds **9** and **10**). As protein structure, considering the docking results and the better resolution of the crystal structure, we have used the 1SA0 tubulin structure. To enhance the quality of the analysis we have chosen a finer parametrization for both ligand and cofactors [16] using a QM approach. We have also evaluated the free binding energy of each selected compounds complexed with tubulin looking to assess if a better correlation with experimental IC_{50} was observed.

In order to better understand the structural nature of the ATIs binding mode, we examined the molecular dynamics trajectories for all the simulations performed. Furthermore, we have also performed the MD calculations on the tubulin/colchicine complex (generated directly from the 1SA0 structure). The well described interactions [17,18] of colchicine (**4**) in its binding site provided us the possibility to evaluate how reliable our own docking/dynamics approach was.

The trajectory analysis showed clearly that the tubulin/colchicine complex reach equilibration in the early stage of simulation, within the first 0.4 ns. The interaction with Cys241β was stable throughout as confirmed by both the low rmsd of the residue (0.55 Å) and the distance from sulfur atom and *p*-methoxy oxygen always lower than 4.5 Å. It should be noted that when this distance increases, the 2C oxygen atom on the ring A of colchicine approaches the sulfur atom to a bond forming distance. Consistently with what reported by Ravelli et al. [12], the H-bond with Val180α had a frequency of formation of 79%. A new H-bond between colchicine NH amidic atom and carbonyl oxygen of Asn100α with a stability of 33% was identified. Also both the oxygen atoms on the colchicine ring C form an H-bond interaction with Nε atom of the Lys353β. However, the rate of formation for these bonds is lower than the other H-bonds examined (O5, 14%; O6, 10%).

Were also observed a series of stable hydrophobic interactions with Leu248β, Leu255β, Met259β and Lys353β. Both leucine residues stabilized the colchicine tri-methoxyphenyl moiety thanks to a staking interaction, while Met259β and Lys353β mainly interacted with the colchicine C ring. The stability of these interactions was evaluated by computing the average rmsd of the involved residues for the whole simulation (respectively 1.64, 1.33 0.63 and

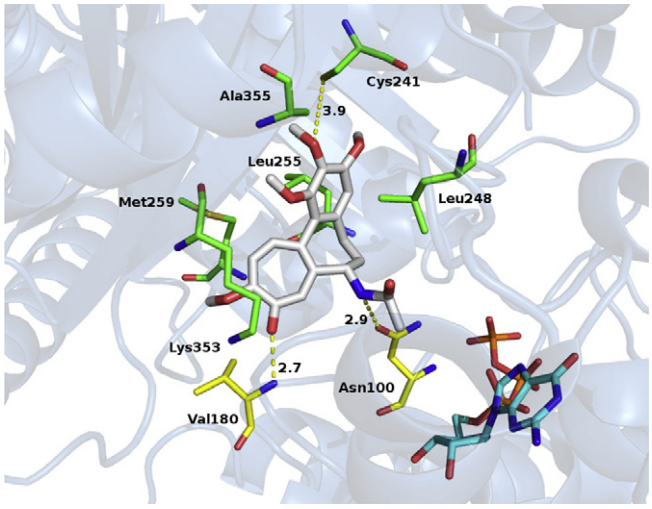

Fig. 3. Putative binding of the colchicine (**4**, white). Tubulin was as cartoon representation. H-bonds are reported as dotted lines, distance in angstrom are also reported; α tubulin residues are reported in yellow; β tubulin residues are reported in green. (For interpretation of the references to colour in this figure legend, the reader is referred to the web version of this article.)

1.20 Å) (Fig. 3). These hydrophobic interactions were extremely important in the stabilization of colchicine binding [11].

On the tubulin/colchicine complex we have also carried out an essential dynamics analysis with the aim to highlight only the motions that describe significant changes in the protein. As we expected the eigenvectors with larger eigenvalues were associated with inter-helical loops fluctuation in particular for the external part of the tubulin structure [20]. No large motion was detectable for the binding site as the porcupine plot [21] (Fig. 4) for the first eigenvector showed [22–25].

The analysis of the IASs training set started with compound **6** which could be defined as the representative compound and the obtained results were used as main comparison with the other analogues. As mentioned above, from the docking results we have observed two possible binding modes for derivative **6** and we have carried out a molecular dynamics simulation for each of the poses. In a previous paper we have reported a similar analysis on the ethyl ester analogue of **6** [9], but the results presented here, considering the finest parametrization and the more accurate simulation performed should be considered more accurate.

The best scored pose from the docking results has also the lowest calculated binding free energy (−8.22 kcal/mol) of the two, while the pose representative of the other cluster results slightly less favorable (−7.70 kcal/mol). Despite the small difference in these values, the accordance between docking score and calculated binding energy suggests that the pose with the ester moiety direct to T7 loop could be considered as the most accurate.

The trajectory of the lowest energy pose of compound **6** showed that the binding conformation was relatively stable (rmsd 1.2 Å) during the whole simulation. The key H-bond with Thr179α had a frequency of formation of 61% showing a high level of stability, also the interaction with Cys241β was stable, although in comparison with what observed for colchicine, the distance between *p*-methoxy oxygen and cysteine sulfur atom increased reaching a maximum value at the end of simulation of about 4.80 Å. As with colchicine, also for derivative **6** a series of stable hydrophobic interactions were observed: mainly with Leu248β and Leu255β which stabilized the tri-methoxyphenyl ring thanks to a staking interaction and between Asn258β side chain and the indole core (Fig. 5).

We then turn our attention to the sulfur bridge and to its structural role. The sulfur linker represents a potential limit of ATIs considering that the metabolic system might oxidize it to sulfone, generating analogues which are inactive as anti tubulin agents. To overcome this issue, we have prepared and tested two series of ATIs analogues where a methylene linker or a carbonyl group replaces the sulfur atom. Generally, these modifications are well tolerated, although the carbonyl analogues appear to be somehow more potent than the corresponding sulfur based analogue. To evaluate the effect of the sulfur replacements on the binding of the ATIs to the colchicine site, we have examined the methylene (**7**) and the carbonyl (**8**) analogues of **6**.

The methylene derivative **7** docked in the binding pocket in a virtually identical conformation of the compound **6** in its best scored pose. The molecular dynamics simulation did not show significant change in the way **7** interact with the binding pocket. The system reached the equilibrium in the early stage of simulation (0.35 ns), the binding pose of **7** was stable (rmsd 1.09 Å). In particular in the last stage of the simulation (Fig. 2S of Supporting

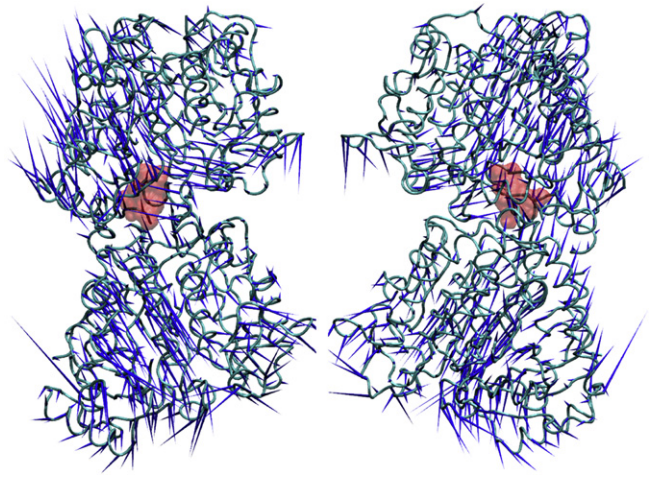

Fig. 4. Porcupine plot Each Cα has a cone attached pointing in the direction of motion described by the eigenvector for this atom.

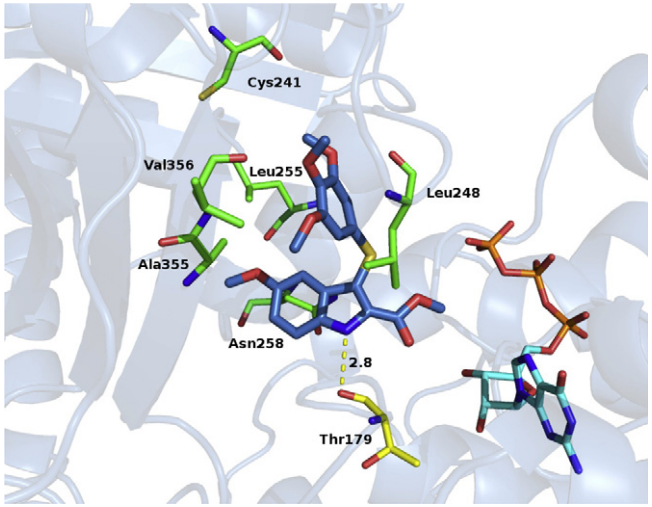

Fig. 5. Putative binding of **6** (blue); H-bonds are reported as yellow dot lines, distance in angstrom is also reported; α tubulin residues are reported in yellow; β tubulin residues are reported in green. (For interpretation of the references to colour in this figure legend, the reader is referred to the web version of this article.)

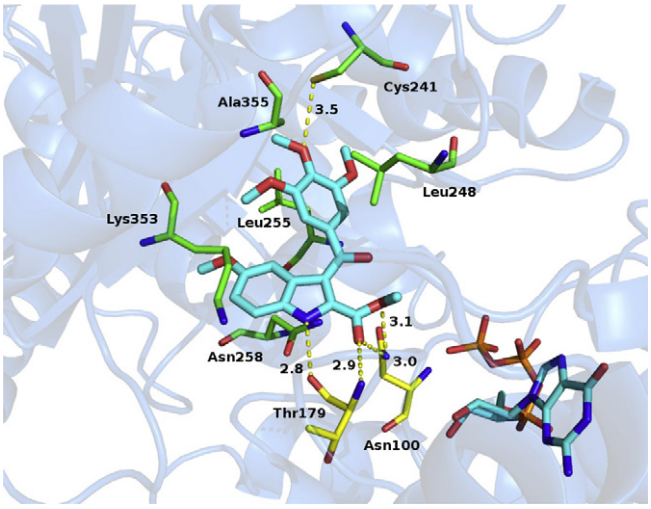

Fig. 6. Putative binding of **8** (cyan); H-bonds are reported as yellow dotted lines, distance in angstrom are also reported; α tubulin residues are reported in yellow; β tubulin residues are reported in green. (For interpretation of the references to colour in this figure legend, the reader is referred to the web version of this article.)

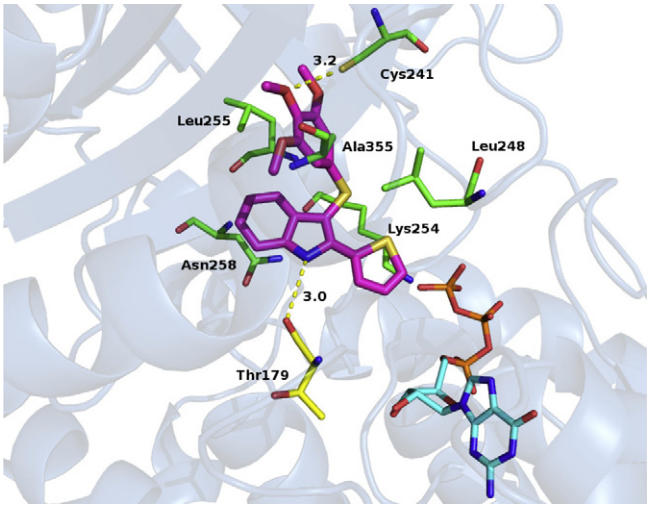

Fig. 8. Putative binding of **10** (magenta). H-bonds are reported as yellow dotted lines, distance in angstrom are also reported; α tubulin residues are reported in yellow; β tubulin residues are reported in green. (For interpretation of the references to colour in this figure legend, the reader is referred to the web version of this article.)

Information) TMP moiety moved far from Cys241β reaching a max distance of 4.80 Å, as observed also for derivative **6**. The key H-bond with Tyr179α was highly stable with a frequency of formation of 88%. Another H-bond, less stable than the above one (rate of formation 17%), was visible with Tyr179α and the oxygen atom of ester group. Also for derivative **7** a series of important hydrophobic interactions were observable with Lys353β, Asn258β and Val181α with the indole ring, Leu248β and Leu255β with the TMP moiety (Fig. 2S of Supporting Information). Overall, from these results, it does not appear that the methylene linker is directly involved in the binding, suggesting that its effect on the conformation of the compound is responsible for the differences in biological activity.

Also the carbonyl analogue **8** shared a similar binding pose with **6** and during the simulation all the crucial interactions were retained. The contact with Cys241β showed the higher rate of stability in terms of both the rmsd of the cysteine residue 0.52 Å and the bond length that after a short period of equilibration (0.25 ns) did not go beyond the 3.9 Å (lower than the distance observed for colchicine) (Fig. 6). The H-bond with Thr179α showed the highest rate of formation 95% for all the ATIs here considered. Furthermore, another H-bond between the side chain ester function carbonyl oxygen and the nitrogen atom of Thr179α (frequency of formation 32%) was observed. Interestingly, both the oxygen atoms of the ester moiety also interact by a series of H-bond with the Asn100α side chain nitrogen atom with a rate of formation of 20% for the carbonyl oxygen and 40% for the alkyl oxygen. The mainly hydrophobic feature of the binding site well arranged both the TMP moiety by contacts primarily with Leu255β, Leu248β and Ala355β and the indole ring stabilized by Lys353β and Asn258β. No direct interactions between the carbonyl bridge atoms were observable. The number and quality of interaction, in particular the close contact between the TMP moiety with Cys241β and the extended hydrophobic interaction, could justify the low IC_{50} value for this analogue. As with the methylene linker, also the carbonyl group does not seem to be directly involved in the binding. It is possible that the increased biological activity generally observed with the analogues with this linker is justified by a water mediated H-bond between the tubulin and **8** (Asn100α is within a suitable distance), however, from the MD simulations we cannot observe a stable interaction of this nature.

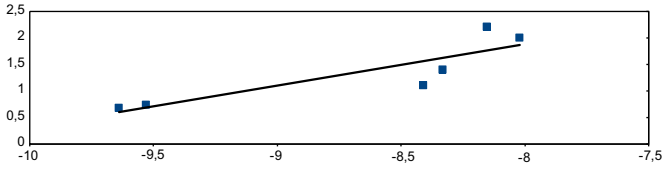

Fig. 7. Correlation of experimental IC_{50} (Y axes) and calculated free binding energy (X axes) for the compounds in Table 2 (r^2 0.74).

At this point, supported by the results obtained and from the good correlation between the calculated binding energy and the IC_{50} (Table 1), we decided to use this *in silico* approach in the design of a novel series of compounds [26]. In particular, we focused our attention to the ester moiety in position 2 of the indole ring (e.g.: **6**, **7**).

In the same way as the sulfur bridge could represent a limit of ATIs by metabolic oxidization, the ester could quickly undergo *in vivo* hydrolysis by the esterases, with consequent loss of activity (the corresponding free acid analogue of **6** loses activity: $IC_{50} > 40$ μM). To overcome this problem we have considered the replacement of the ester group with some bioisosteric heterocycle rings. A new series of docking runs were performed on newly designed compounds, and MD simulations were performed on the two best scored analogues, **9** and **10**. The low calculated binding energy for these compounds (Table 1 and Fig. 7) encouraged us to prepare and evaluate this series of analogues, which proved to be highly potent (Table 1) [26].

Derivatives **9** and **10** showed a consistent binding mode close to that observed for other ATIs and for compound **6** in its best scored pose. For both compounds the main interactions were retained: the distances to the Cys241β were always under 3.8 Å (similar to what observed with derivative **8**); the H-bonds with Tyr179α had a rate of formation of 80% for **9** and 55% for **10**. Furthermore, all the hydrophobic contacts observed for the other analyzed ATIs were retained. In addition to these interactions some other peculiar binding features for both compounds were observed. For derivative **9** another H-bond linking the pyrrole nitrogen atom still with Thr179α with a rate of formation of 35% is established (Fig. 3S of Supporting Information). Instead, for derivative **10** was observed an important hydrophobic interaction between Lys254β and the thiophene ring (Fig. 8).

3. Conclusion

We have reported a series of molecular modelling studies on the ATIs series, which proved to be useful in the design of novel, more potent analogues. Although a model based solely on docking and scoring could not be considered accurate yet, the molecular dynamics simulations on different tubulin/ATIs complexes proved to be extremely useful in understanding the structural nature of the binding of these compounds to tubulin. The TMP moiety was already known to be of crucial importance to achieve a good biological activity and our studies confirmed this observation. From the MD simulation it is possible to note how the average contact distance between the TMP and Cys241β increases when we move from the most active to the least active analogues in the series studied. The key role of H-bond between the indole nitrogen atom and Thr179α amide group was also confirmed by molecular dynamics simulation: we have never observed rate of formation of this H-bond lower than 55%.

Less clear is the role of the linker group. Both docking and molecular dynamics simulations did not specify a direct structural role for this position in the binding of the ATIs to tubulin.

Finally, important information that emerged from our results, which was used in the design of a novel series of potent ATIs analogues, regards the position 2 of the indole core. The ester function, that in previous studies was considered crucial for the inhibition of tubulin polymerization, can indeed be replaced by small heterocyclic groups, preserving, if not enhancing, the biological activity. The good correlation between the *in silico* results and the experimental data has given us confidence in the accuracy and predictive properties of our modelling approach, which, as we already seen it, would be an extremely useful tool in the design of novel, more potent ATIs in the near future.

4. Experimental

All molecular modelling studies were performed on a MacPro dual 2.66GHz Xeon running Ubuntu 9. The tubulin structure was downloaded from the PDB data bank (http://www.rcsb.org/– PDB ID: 1SA0 [12], 3KHC and 3KHE [11]. Hydrogen atoms were added to the protein, using Molecular Operating Environment (MOE) 2007.09 [27], and minimized keeping all the heavy atoms fixed until an RMSD gradient of 0.05 kcal mol^{-1} $Å^{-1}$ was reached. Ligand structures were built with MOE and minimized using the MMFF94x forcefield until an RMSD gradient of 0.05 kcal mol^{-1} $Å^{-1}$ was reached. The docking simulations were performed using Plants1.1 [14] and GLIDE [15]. Molecular dynamics was performed with AMBER 9 package [28] on 1SA0 crystal structure. The minimized structure was solvated in a periodic octahedron simulation box using TIP3P water molecules, providing a minimum of 10 Å of water between the protein surface and any periodic box edge. Sodium ions were added to neutralize the charge of the total system. The water molecules and sodium ions were energy minimized keeping the coordinates of the protein–ligand complex fixed (1000 cycle) then the whole system was minimized (5000 cycle). Following minimization, the entire system was heated to 298 K (10 ps). The production simulation was conducted at 298 K (time step 0.002 ps) with isotropic position scaling (ntp = 1) using as pressure relaxation time of 2.0 ps. The periodic boundary condition was settled. The Particle mesh ewald (PME) was used while the size of the charge grid was chosen by the program and the spline interpolation order settled to default. The used cutoff was 8 Å. Shake bond length condition was used (ntc = 2). The polyphorylated compounds (GTP and GDP) were parametrized using orbital molecular calculation at the RHF/6–31 + G^* level [16]. Compounds were parametrized by Gamess [29,30] at the HF/6–31 + G^* level. Trajectories analysis: RMSD, PCA, Clustering and H-bond rate of formation were carried out by Ref. [19] program, visual inspection was carried out by VMD [24]. The free binding energy (△G) reported in Table 1 were calculated by Refs. [31,32]. The images in the manuscript were created with Pymol [33].

Acknowledgments

This research was supported by Italian PRIN 2008 grant n. 200879X9N9, and Sapienza PRU 2009. A.C. thanks IP – FCB for his “Borsa di Studio per Ricerche Estero”. A.C. thanks Dr. Enrico Purissima for help and useful suggestions.

Appendix. Supplementary material

Supplementary data associated with this article can be found, in the online version, at doi:10.1016/j.ejmech.2011.05.020.

References

[1] A.M. Jordan, L. Wilson, Nature Rev. 4 (2004) 253–260.
[2] A.M. Jordan, J.A. Hadfield, N.J. Lawrence, A.T. McGown, Med. Res. 18 (1998) 259–296.
[3] E. Nogales, M. Whittaker, R.A. Milligan, K.H. Downing, Cell 96 (1999) 79–88.
[4] J.H. Nettles, H. Li, B. Cornett, J.M. Krahn, J.P. Snyder, K.H. Downing, Science 305 (2004) 866–869.
[5] M. Sridhare, M.J. Macapinlac, S. Goel, D. Verdier-Pinard, T. Fojo, M. Rothenberg, D. Colevas, Anticancer Drugs 15 (2004) 553–555.
[6] D. Calligaris, P. Verdier-Pinard, F. Devred, C. Villard, D. Braguer, D. Lafitte, Cell. Mol. Life. Sci. 67 (2010) 1089–1104.
[7] G. De Martino, G. La Regina, A. Coluccia, M.C. Edler, M.C. Barbera, A. Brancale, E. Wilcox, E. Hamel, M. Artico, R. Silvestri, J. Med. Chem. 47 (2004) 6120–6123.
[8] G. La Regina, S. Sarkar, R. Bai, M.C. Edler, A. Coluccia, F. Piscitelli, V. Gatti, V. Palermo, C. Mazzoni, E. Hamel, A. Brancale, E. Novellino, R. Silvestri, J. Med. Chem. 52 (2009) 7512–7527.
[9] G. De Martino, M.C. Edler, G. La Regina, A. Coluccia, M.C. Barbera, A. Brancale, E. Hamel, M. Artico, R. Silvestri, J. Med. Chem. 49 (2006) 947–954.
[10] G. La Regina, M.C. Edler, A. Brancale, A. Coluccia, F. Piscitelli, E. Hamel, E. Novellino, M. Artico, R. Silvestri, J. Med. Chem. 50 (2007) 2865–2874.
[11] A. Dorleans, B. Gigant, R.B. Ravelli, P. Mailliet, V. Mikol, M. Knossow, PNAS, USA 106 (2009) 13775–13779.
[12] R.B. Ravelli, B. Gigant, P.A. Curmi, I. Jourdain, S. Lachkar, A. Sobel, M. Knossow, Nature 428 (2004) 198–202.
[13] FlexX 3.0. BioSolveIT GmbH, Sankt Augustin, Germany, http://www.biosolveit.de.
[14] O. Korb, T. Stützle, T.E. Exner, Lecture Notes Comput. Sci. 4150 (2006) 247–258.
[15] R.A. Friesner, R.B. Murphy, M.P. Repasky, L.L. Frye, J.R. Greenwood, T.A. Halgren, P.C. Sanschagrin, D.T. Mainz, J. Med. Chem. 21 (2006) 6177–6196.
[16] K.L. Meagher, L.T. Redman, H.A. Carlson, J. Comput. Chem. 24 (2003) 1016–1032.
[17] T.L. Nguyen, C. McGrath, A.R. Hermone, J.C. Burnett, D.W. Zaharevitz, B.W. Day, P. Wipf, E. Hamel, R. Gussio, J. Med. Chem. 48 (2005) 6107–6116.
[18] R. Bai, D.G. Covell, X.F. Pei, J.B. Ewell, N.Y. Nguyen, A. Brossi, E. Hamel, J. Biol. Chem. 22 (2000) 40443–40452.
[19] http://ambermd.org/#AmberTools.
[20] A. Amadei, A.B.M. Linssen, H.J.C. Berendsen, Proteins 17 (1993) 412–425.
[21] A. Rajan, P.L. Freddolino, K. Schulten, PLos ONE 5 (2010) 1–12.
[22] C.P. Barrett, B.A. Hall, M.E.M. Noble, Acta Crystallogr. D 60 (2004) 2280–2287.
[23] E. Lindahl, B. Hess, D.V.D. Spoel, J. Mol. Mod. 7 (2001) 306–317.
[24] B.L. De Groot, D.M. Van Aalten, R.M. Scheek, A. Amadei, G. Vriend, H.J. Berendsen, Proteins 29 (1997) 240–251.
[25] W. Humphre, A. Dalke, K. Schulten, J. Mol. Graph. 14 (1996) 27–38.
[26] G. La Regina, T. Sarkar, W. Rensen, A. Coluccia, R. Bai, F. Piscitelli, M.C. Edler, V. Gatti, P. Campiglia, A. Brancale, E. Hamel, P. Lavia, E. Novellino, R. Silvestri, J. Med. Chem., submitted for publication.
[27] Molecular Operating Environment (MOE 2007.09), Chemical Computing Group, Inc., Montreal, Quebec, Canada, http://www.chemcomp.com.
[28] D.A. Case, T.E. Cheatham III, T. Darden, H. Gohlke, R. Luo, K.M. Merz Jr., A. Onufriev, C. Simmerling, B. Wang, R. Woods, J. Comput. Chem. 26 (2005) 1668–1688.
[29] M.W. Schmidt, K.K. Baldridge, J.A. Boatz, S.T. Elbert, M.S. Gordon, J.H. Jensen, S. Koseki, N. Matsunaga, N.Y. Nguyen, S. Su, T.L. Windus, M. Dupuis, J.A. Montgomery, J. Comput. Chem. 14 (1993) 1347–1363.
[30] M.S. Gordon, M.W. Schmidt, Advances in electronic structure theory: GAMESS a decade later. in: C.E. Dykstra, G. Frenking, K.S. Kim, G.E. Scuseria (Eds.), Theory and Applications of Computational Chemistry: the First Forty Years. Elsevier, Amsterdam, 2005, pp. 1167–1189.

[31] Q. Cui, T. Sulea, J.D. Schrag, C. Munger, M.N. Hung, M. Naïm, M. Cygler, E.O. Purisima, Molecular dynamics-solvated interaction energy studies of protein–protein interactions: the MP1–p14 scaffolding complex, J. Mol. Biol. 379 (2008) 787–802.
[32] M. Naïm, S. Bhat, K.N. Rankin, S. Dennis, S.F. Chowdhury, I. Siddiqi, P. Drabik, T. Sulea, C. Bayly, A. Jakalian, E.O. Purisima, J. Chem. Inf. Model. 47 (2007) 122–133.
[33] PyMOL, DeLano Scientific LLC, San Carlos, California, U.S.A. www.pymol.org.